REFERENCES

[1] Moyal, J. E.
The general theory of stochastic population processes.
Acta Mathematica, **108** (1962), 1–31.

[2] Wilf, H. S.
Generating Functionology. New York: Academic Press, 1994.

[3] Streit, R.
The probability generating functional for finite point processes, and its application to the comparison of PHD and intensity filters.
Journal on Advances in Information Fusion, **8**, 2 (Dec. 2013).

[4] Streit, R.
Poisson Point Processes—Imaging, Tracking, and Sensing.
New York: Springer, 2010.

[5] Mahler, R. P. S.
Multitarget Bayes filtering via first-order multitarget moments.
IEEE Transactions on Aerospace and Electronic Systems, **39** (2003), 1152–1178.

[6] Erdinc, O., Willett, P., Bar-Shalom, Y.
The bin-occupancy filter and its connection to the PHD filters.
IEEE Transactions on Signal Processing, **57**, 11 (2009), 4232–4246.

[7] Chen, X., Tharmarasa, R., Kirubarajan, T., and Pelletier, M.
Integrated clutter estimation and target tracking using Poisson point process. *Proceedings of SPIE*, vol. 7445, 2009.

[8] Streit, R., and Stone, L.
Bayes derivation of multitarget intensity filters. *Proceedings of the 11th International Conference on Information Fusion*, Cologne, Germany, July 2008.

[9] Streit, R.
A Technique for Deriving Multitarget Intensity Filters Using Ordinary Derivatives.
Journal of Advances in Information Fusion, **9**:1, in press.

[10] Mahler, R. P. S.
Statistical Multisource-Multitarget Information Fusion.
Boston: Artech House, 2007.

[11] Cressie, N., and Wikle, C.
Statistics for Spatio-Temporal Data. New York: Wiley, 2011.

[12] Baddeley, A.
Spatial point processes and their applications. In W. Weil (Ed.),
Stochastic Geometry (Lecture Notes in Mathematics), vol. 1892. Berlin: Springer-Verlag, 2007, pp. 1–75.

[13] Griewank, A., Lehmann, L., Leovey, H., and Zilberman, M.
Automatic evaluations of cross-derivatives.
Mathematics of Computation, **83**, 285 (Jan. 2014), 251–274.

[14] Bozdogan, O., Streit, R., and Efe, M.
Reduced Palm intensity for track extraction.
Proceedings of the International Conference on Information Fusion, Istanbul, July 2013.

ROY STREIT,
Metron, Inc.
1818 Library St.
Reston, VA 20190
E-mail: (r.streit@ieee.org)

Real-Time Wind Speed Estimation and Compensation for Improved Flight

This paper presents the development and experimental validation of a prototype system for online estimation and compensation of wind disturbances onboard small Rotorcraft unmanned aerial systems (RUAS). The proposed approach consists of integrating a small pitot-static system onboard the vehicle and using simple but effective algorithms for estimating the wind speed in real time. The baseline flight controller has been augmented with a feed-forward term to compensate for these wind disturbances, thereby improving the flight performance of small RUAS in windy conditions. The paper also investigates the use of online airspeed measurements in a closed-loop for controlling the RUAS forward motion without the aid of a global positioning system (GPS). The results of more than 80 flights with a RUAS confirm the validity of our approach.

I. INTRODUCTION

Rotorcraft unmanned aerial systems (RUAS) are becoming popular and have been increasingly used for a wide range of civilian and military applications. Despite the progress in automatic flight control and the maturity of RUAS technology, many control challenges still remain, such as accurate and robust control of RUAS in windy conditions. This is a major problem for small multirotor UAS, such as the popular quadrotor platforms, and a limiting factor for many applications. Their small size and limited propulsion power make them very sensitive to wind gusts and turbulent atmosphere that can result in several meters of position error and unstable flight or vehicle crash in some cases. Wind disturbance rejection is thus important for many applications, especially the ones that require flying close to objects and obstacles.

The work presented in this paper addresses this problem by investigating the feasibility and effectiveness of online estimation and compensation of the wind speed onboard small RUAS for improved flight performance in windy conditions. The main contributions of this paper are 1) the development and evaluation of an airspeed-based system for online estimation of wind speed onboard small unmanned rotorcraft; 2) the design and implementation of a simple but effective feed-forward controller for wind gust compensation, thereby providing stable and accurate flight in windy conditions; 3) the successful flight tests of RUAS forward motion control using airspeed measurements without a global positioning system (GPS); and 4) the closed-loop flight testing of the developed system in outdoor environments under different wind conditions and for different maneuvers.

Manuscript received April 23, 2012; revised January 4, 2013, May 23, 2013; released for publication September 5, 2013.

DOI. No. 10.1109/TAES.2014.120236.

Refereeing of this contribution was handled by I. Hwang

There are very few works that dealt with wind speed estimation onboard RUAS or flight control in windy conditions. Indeed, most works on in-flight estimation of wind speed have been done with fixed-wing UAS [1, 2]. In [1], an extended Kalman filter is used to estimate the wind speed and direction onboard a fixed-wing UAS. The algorithm fuses data from GPS and pitot tube at different headings, such as during a banking turn and circular maneuvers. Flight test results showed that the method works well in real time. However, these wind measurements were not used in the control loop. A similar wind estimation system is presented in [2] and verified in flight tests but without using these estimates in the flight controller.

Wind speed estimation on helicopters and RUAS is very challenging due to adverse flow fields from the rotors. This is even more challenging for small RUAS traveling at low speed because airspeed readings from the pitot-static system are not reliable and accurate at low speeds. Most reported results about wind speed estimation and/or compensation onboard RUAS are from simulations or from very modest indoor flight tests. For example, the research described in [3] is similar to our work where a feed-forward controller was used to reject wind disturbances on a small autonomous helicopter. The obtained results from indoor flights are promising, but wind estimation was performed by a ground-based anemometer (i.e., off-board) that was placed near the fan. Therefore, some researchers have investigated an alternative algorithmic approach for estimating wind disturbances onboard rotorcraft without using a pitot-static system. Generally, the idea is to assume a disturbance model of wind gust [4] and to identify the disturbance model parameters using an observer. In [5], an active disturbance rejection control based on a nonlinear extended state observer is proposed to estimate the wind disturbances and validated in simulations only. A backstepping-based controller is also used in [6] to estimate the external disturbances and to stabilize the position of a ducted fan UAS in wind gusts. A proportional-derivative controller is presented in [7] for the heave dynamics that exploits wind gust estimates to improve the disturbance attenuation capability. A robust nonlinear controller is presented in [8] to stabilize the quadrotor platform in presence of cross winds. The proposed controller was demonstrated in indoor environment with lateral wind gusts produced by the fan. Therefore, the difference between our system and most other works such as those in [1, 2, 3] is in using the wind speed estimates in the closed-loop flight controller. Furthermore, the system has been demonstrated in extensive outdoor flights and in real-world conditions.

The organization of this paper is as follows: Section II presents the developed wind estimation system, including hardware and algorithms. Section III presents an overview of the control architecture. The experimental flight results are presented in Section IV. Section V presents the control of forward speed using airspeed measurements only, followed by the conclusion of the paper in Section VI.

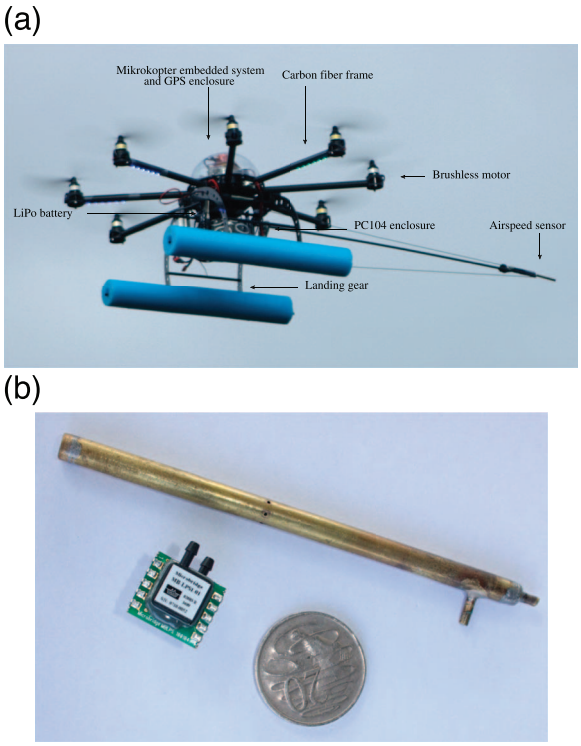

Fig. 1. Wind estimation system onboard small unmanned rotorcraft (Helix8). (a) Integrated system onboard Helix8. (b) Pitot tube and pressure sensor used for airspeed measurement on Helix8.

II. INTEGRATION AND EVALUATION OF THE WIND ESTIMATION SYSTEM

A. Hardware of the Estimation System

A pitot-static sensor is the core of our wind speed estimation system. It is usually used to measure the airspeed onboard manned and unmanned fixed-wing aircraft. There exists a relationship between the velocity of the fluid V_{pitot} and the airspeed V_a for small angle of attack α and small side slip angle β, given by [1]

$$V_{pitot}^2 \simeq \|V_a\|^2 cos\alpha\, cos\beta \Rightarrow V_a \simeq \frac{|V_{pitot}|}{\sqrt{cos\alpha\, cos\beta}}. \quad (1)$$

A second-order low-pass digital filter with cutoff frequency of 2.0 Hz has been also implemented to reduce noise in the data acquisition system.

Fig. 1(b) shows the pitot-static tube and the differential air pressure sensor that we have used in this research, along with an Australian 20-cent coin (28.52-mm diameter) for a size comparison. The system has been integrated and tested onboard a small octorotor UAS, as shown in Fig. 1(a).

Airspeed is generally measured onboard fixed-wing aircraft by mounting the pitot tube either on the front nose of the aircraft or onto the wing. Generally, it is pointing forward to measure airspeed in the longitudinal x-axis of the aircraft that usually coincides with the flight direction.

However, it is extremely difficult to find a suitable position on a rotorcraft platform due to its small size and the downwash of the rotor system. The configuration that presented good trade-off between the accuracy of airspeed measurements and the distance from the rotor system is the one shown in Fig. 1(a). The pitot tube was aligned with the longitudinal x-axis of the platform to optimize its performance during longitudinal forward flights.

REMARK 1: The flight-tested airspeed measurement system (pressure sensor, pitot tube, and boom) is a first prototype that was built in a short time to provide a proof of concept. It weighs about 200 g, and the long boom (50 cm) can make it somewhat impractical for small-scale rotorcraft and negate some of their advantages, such as compactness, mechanical simplicity, etc. However, it is possible to build a more professional and much lighter (<50 g) version of the system that can be easily mounted and unmounted from the rotorcraft with negligible misalignment errors.

B. Wind Speed Estimation

Airspeed measurements are obtained in real-time onboard the RUAS according to (1). It is well known that the vector sum of airspeed and wind speed is equal to the ground speed, given by

$$\vec{V}_g = \vec{V}_a + \vec{V}_w \,, \tag{2}$$

where $\vec{V}_g$ is the ground speed of the rotorcraft, $\vec{V}_a$ is the airspeed vector, and $\vec{V}_w$ is the wind speed.

To estimate the three-dimensional (3D) vector of the wind speed $\vec{V}_w$ (or wind speed magnitude and direction), one needs to measure the airspeed vector $\vec{V}_a$ in three dimensions, which is challenging. A full-scale aircraft measures the airspeed in the forward direction only, and, similarly here, the airspeed is only estimated in the forward direction along the x-axis. Therefore, in the general case, given instantaneous measurements of airspeed and ground speed in the longitudinal x-axis, the longitudinal component of the wind speed along the x-axis can be computed by projecting (2) on the longitudinal x-axis as follows:

$$V_{g_x} = V_{a_x} + V_{w_x} \;\Rightarrow\; V_{w_x} = V_{g_x} - V_{a_x}. \tag{3}$$

It is important to note that the system will still estimate the longitudinal component of the wind speed in most cases without any assumption. This is the most important component that is critical for many applications, especially for control purposes. However, if the wind direction is parallel and opposite to the longitudinal x-axis of the RUAS and the RUAS is flying forward, then (3) can be written as

$$V_w = V_a - V_g, \tag{4}$$

where V_w, V_g, and V_a are, respectively, the total magnitudes of the wind speed vector, the ground speed vector, and the airspeed vector (i.e., $V_w = \|\vec{V}_w\|$, $V_g = \|\vec{V}_g\|$ and $V_a = \|\vec{V}_a\|$).

For the testing and evaluation of this first prototype of the pitot-static system, we assume that the wind direction is known a priori (determined by a ground-based weather station) and the rotorcraft is flying forward along its longitudinal x-axis.

The first assumption is made to maximize the airspeed and wind speed along the pitot-static sensor (i.e., longitudinal direction) for better evaluation of the system. As mentioned, the system will still estimate the longitudinal component of the wind speed along the x-axis even if this assumption is not met. The second assumption is not very restrictive because most aircraft and rotorcraft tend to fly forward along the longitudinal x-axis. However, for some applications, it would be useful to estimate the 3D wind field (i.e., both wind speed and direction). This can be done by using a multisensor configuration in which each pitot-static sensor is pointing in a different direction or by using one sensor with special flight modes.

C. Experimental Evaluation of the Airspeed and Wind Speed Estimation System

The objectives of these tests and experiments are to 1) evaluate the performance of the pitot-static system for measuring the airspeed (1) onboard the RUAS; and 2) evaluate the accuracy of wind speed estimation (4) onboard the RUAS.

1) *Evaluation of Airspeed Measurement*: Because it was very difficult to integrate a ground truth system into a small RUAS to measure the true airspeed, we have performed the flight tests in calm weather conditions (no wind) and used the GPS ground speed to evaluate the accuracy and reliability of the pitot-static sensor during flight. Indeed, in calm weather conditions where the wind speed is negligible ($V_w \approx 0$), the airspeed should be equal to the ground speed, i.e., $V_a \approx V_g$. A number of flight experiments were conducted in calm wind conditions at different forward speeds and heights and for different maneuvers or trajectory patterns. A subset of experimental results is shown in Figs. 2(a), 2(b).

It can be seen in Figs. 2(a), 2(b) that the airspeed measurements match the GPS ground speed data with some small errors. These are very satisfactory results with an average error of about 0.737 m/s and a maximum error of about 1.803 m/s. These errors between airspeed and ground speed measurements can be due to many factors, including atmospheric disturbances (i.e., the wind speed is not exactly zero as assumed), delays in GPS measurements, etc. It is also important to note that airspeed measurements are not accurate and reliable at low speeds and/or backward flights as expected. Indeed, airspeed measurements are noisy when the rotorcraft ground speed is less than 1.0 m/s or flying backwards ($V_x < 0$), as seen in Figs. 2(a), 2(b).

2) *Evaluation of Wind Speed Estimation*: Several experiments were performed in windy conditions to assess

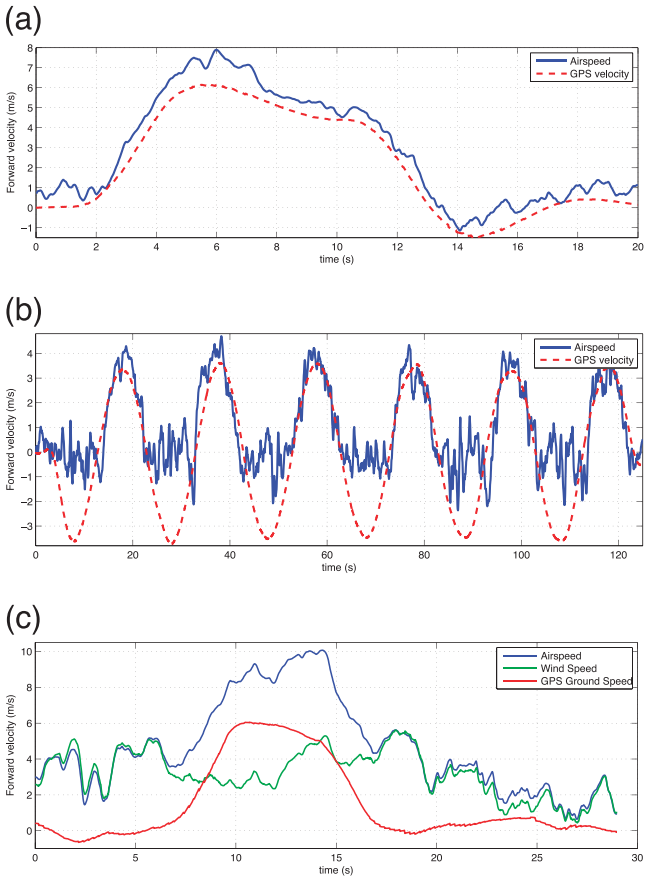

Fig. 2. Evaluation of airspeed measurements and wind speed estimation through flight tests. (a) Airspeed measurements validation by comparison to GPS ground speed during forward flight test. (b) Comparison between airspeed measurements and GPS ground speed during sinusoidal flight trajectory. (c) Estimation of wind speed as difference between airspeed and GPS ground speed during forward flight in windy conditions.

the effectiveness and reliability of the pitot-static system to estimate the wind speed onboard small RUAS. We have used a weather station that provides estimates of the wind speed and direction on the ground with an update rate of one measurement every 60.0 s. In addition to the weather station, we have also used an anemometer (handheld wind meter) to have real-time estimates of the wind speed as well as wind gusts. We have used these weather station and anemometer measurements as pseudoground truth to just get an approximate idea of the average wind speed.

Fig. 2(c) shows the results of a flight test in which the rotorcraft was commanded to fly forward along a straight trajectory opposite to the wind direction.[1] This time the airspeed measurements are different from the GPS ground speed that indicates that the rotorcraft was flying against wind, and the difference between airspeed and ground speed (i.e., the difference between blue curve and red curve) represents the wind speed; see (4). These wind speed estimates obtained onboard the rotorcraft are in agreement with the wind speed measurements of the

[1]The wind direction is determined before takeoff by the weather station.

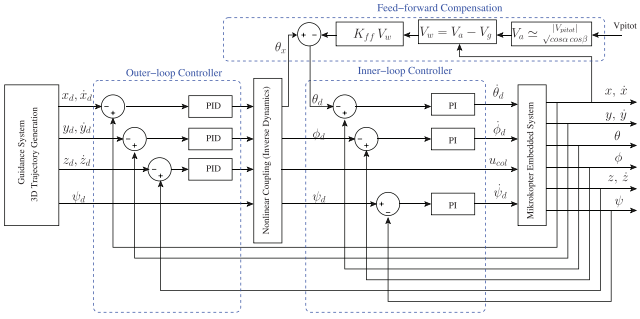

Fig. 3. Block diagram of control architecture.

weather station and the anemometer. Indeed, the measured wind speed at the base station during this flight test was between 2.0 m/s and 4.0 m/s, with wind gusts of about 6.0 m/s. More experimental results about wind speed estimation are presented in Section IV. The experimental results of several flight tests with different weather conditions showed that it is possible to reliably estimate the wind speed onboard small rotorcraft for airspeeds that are higher than 1.0 m/s.

III. AUGMENTED FLIGHT CONTROLLER

We have implemented a hierarchical flight controller with an inner loop and an outer loop to use as a baseline flight controller. Fig. 3 shows the controller architecture onboard the RUAS that we have used for flight tests.[2] The compensation mechanism proposed in this paper is based on a simple but effective feed-forward term that is proportional to the wind speed estimated onboard the RUAS. The outer-loop controller responsible for motion control along the longitudinal x-axis has been augmented as follows:

$$\theta_d = \begin{cases} -K_{ff}\, V_w + \theta_x & V_w > 2.0 \\ \theta_x & V_w \leq 2.0 \end{cases}, \qquad (5)$$

where θ_d is the total desired or reference pitch angle sent to the inner loop, θ_x is the *feedback* component of the reference pitch angle that is computed by the baseline outer-loop controller, and K_{ff} is the feed-forward gain. Therefore, $-K_{ff}\, V_w$ represents the feed-forward component of the reference pitch angle that is used for wind disturbance compensation along the x-axis. As discussed in Section II-C, the compensation mechanism is enabled only when the wind speed exceeds a preset threshold of 2.0 m/s due to signal-to-noise ratio of the airspeed and wind speed measurements. When the estimated wind speed is less than this threshold, it means that the induced wind disturbance is very small, and the baseline controller can reject it without the need for the

[2]Although the platform has eight rotors, it is still an underactuated system with only four control inputs for the system dynamics that we have considered. In our implementation, we kept the MikroKopter internal controller for angular rates stabilization and we have considered the following four control inputs for our system: 1) desired pitch rate, 2) desired roll rate, 3) desired yaw rate, and 4) thrust.

compensation mechanism. In our flight experiments, the feed-forward gain K_{ff} was set to 1.0°s/m. This value of K_{ff} was chosen empirically and obtained after observing the pitch angle during manual flight in windy conditions.

IV. EXPERIMENTAL FLIGHT RESULTS

The developed system (hardware and software) has been implemented onboard the rotorcraft and tested in closed-loop flights. The flight tests were performed outdoors in different weather conditions and for several flight maneuvers including hover, forward flight, sinusoidal trajectory tracking, circular trajectory tracking, and way point navigation. A total of 84 flight tests were conducted to confirm the reliability but also the limitations of the system. The experimental flight tests are divided into three categories:

1) Baseline flight controller in calm weather conditions: the objective of these flight tests is to evaluate the performance of the baseline controller in calm conditions.

2) Baseline flight controller in windy conditions: the objective of these series of flight tests is to show that small RUAS are vulnerable to wind disturbances and the performance of flight controllers degrade if these disturbances are not estimated and compensated.

3) Augmented flight controller in windy conditions: this last set of flight experiments aims to prove the effectiveness of the developed system for estimating and rejecting wind disturbance onboard small rotorcraft.

A. Performance of the Baseline Controller in Calm Conditions

Flight test results of the Helix8 RUAS using baseline controller are shown in Fig. 4 for hovering and trajectory tracking. The experimental results of this first phase of flight testing show that the implemented baseline controller performs well and provides accurate hovering and trajectory tracking in calm weather conditions with maximum position errors of about ± 0.5 m and ± 2.0 m, respectively.

B. Performance of the Baseline Controller in Windy Conditions

In the second phase, we have performed several flight tests with the baseline flight controller in relatively windy conditions, and some experimental results are shown in Fig. 5. The position error along the x-axis as well as onboard estimates of the wind speed are plotted in Fig. 5(a). It can be seen that the maximum position error reached approximately -5.0 m when the vehicle was subject to a wind gust of about 11.0 m/s. This position error is significantly higher than the one (about 0.5 m) obtained for a similar hover maneuver in calm weather conditions (see Fig. 4 for comparison).

The baseline controller was also evaluated in these windy condition for a forward flight maneuver, and some of the experimental results of these flights, where the

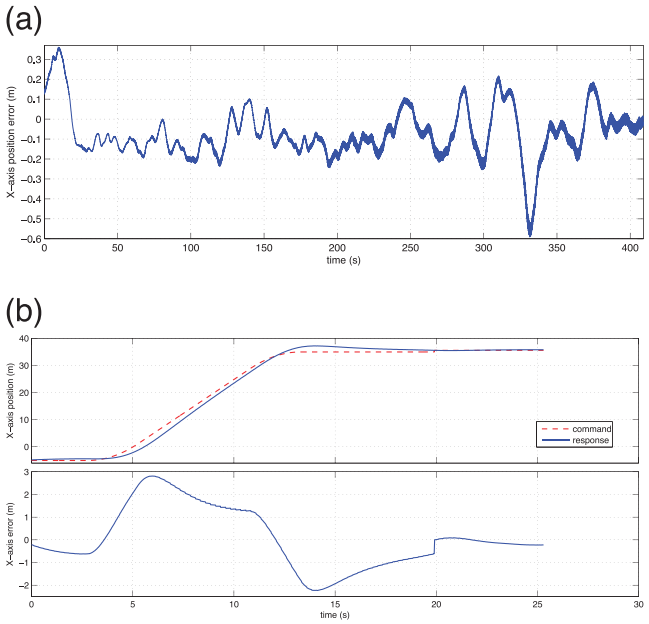

Fig. 4. Baseline controller performance in calm weather conditions.(a) Longitudinal axis position error using baseline controller during hover flight. Note that noise in plot is due to propagation phase of Kalman filter for GPS/INS fusion.(b) Forward flight trajectory and longitudinal axis position error using baseline controller in calm weather conditions. Reference forward velocity of 5.0 m/s was commanded during this flight test.

trajectory tracking and position error in the x-axis, as well as onboard wind estimates are plotted, are shown in Fig. 5(b). The maximum and root mean square error (RMSE) of the position error in the x-axis for this forward flight are about 6.5 m and 3.15 m, respectively. These position errors are, again, far greater than the ones obtained in calm conditions (see Fig. 4(b) for comparison).

The experimental results obtained in these series of flight tests prove that small rotorcraft equipped with a baseline flight controller, such as most commercial ones, are very vulnerable to wind. Therefore, one needs to consider these effects and position errors when operating small RUAS near structures and objects in relatively windy conditions.

REMARK 2: When tuning the flight controller in the first phase of flight tests (Section IV-A), the control gains of the outer-loop position controller were set to high values (tight controller) to maximize the ability of the baseline controller to reject wind disturbances. However, even with these strong/high gains, wind gusts of about 10.0 m/s were able to induce about 5.0 m error in position control during hovering; see Fig. 5.

C. Performance of the Augmented Flight Controller in Windy Conditions

It has been experimentally shown that the performance of flight controllers degrade in windy conditions (see Section IV-B). In this phase, we evaluate the performance of the augmented flight controller in windy

TABLE I
RMSE and Maximum Error in X-Axis in the Body Coordinate Frame

			With Compensation		Without Compensation		
	Time (s)	Maximum Wind Speed (m/s)	RMSE in X-Axis (m)	Maximum Error in X-Axis (m)	RMSE in X-Axis (m)	Maximum Error in X-Axis (m)	Improvement (%)
Hover 1	245.1	9.6290	0.3407	0.8048	0.8243	1.4946	58.73
Hover 2	351.5	11.1878	0.7601	1.9981	1.7083	2.2109	55.50
Hover 3	358.6	10.5565	0.4343	1.3130	1.1862	1.5772	63.41
Hover 4	365.4	8.9372	0.4243	0.7805	0.6470	1.7546	34.46
Hover 5	286.3	5.6712	0.3361	0.6947	0.3961	0.7318	16.66
Forward 1	286.3	8.2832	1.2594	1.1718	1.7733	2.8291	30.0
Forward 2	261.5	10.72	0.4297	0.8282	1.2347	1.5348	65.17

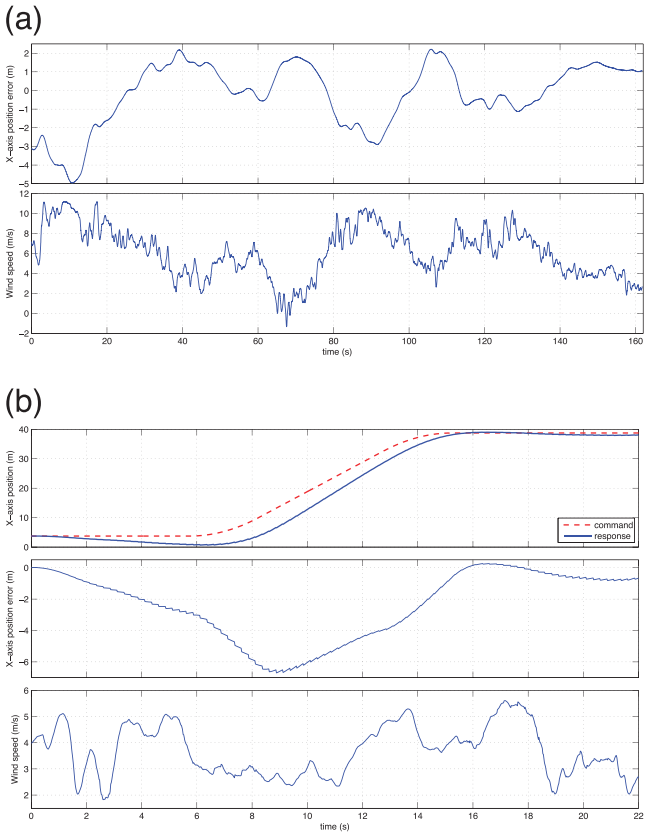

Fig. 5. Baseline controller performance in windy conditions.(a) Onboard wind speed estimates and position tracking errors in longitudinal x-axis during hover flight using baseline controller. (b) Onboard wind speed estimates and position tracking errors in longitudinal x-axis during forward flight using baseline controller. Reference forward velocity of 5.0 m/s was commanded during this flight test.

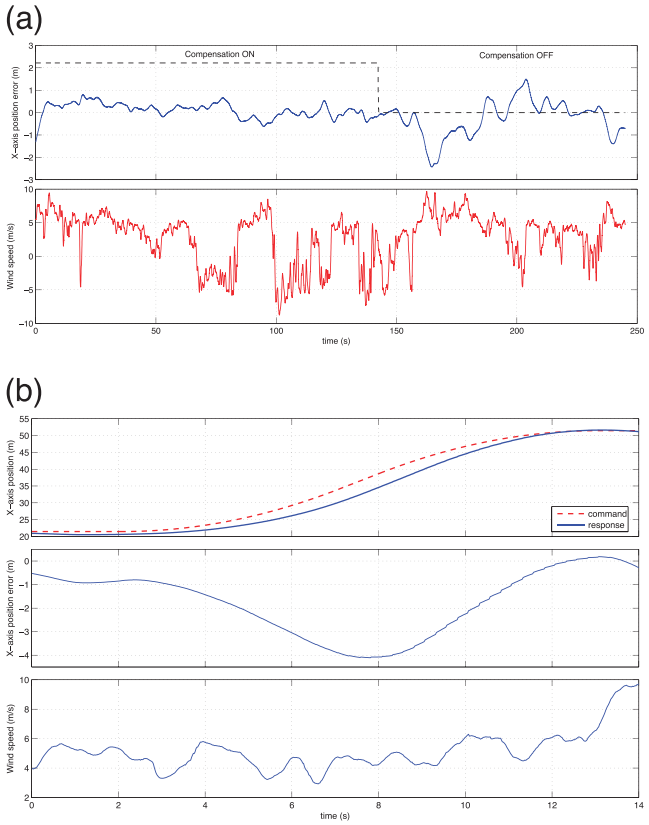

Fig. 6. Flight test results with and without feed-forward compensation in windy conditions.(a) Onboard wind speed estimates and position tracking errors in longitudinal x-axis with and without feed-forward compensation. (b) Onboard wind speed estimates and position tracking errors in longitudinal x-axis during forward flight in windy conditions using augmented flight controller (i.e., with feed-forward compensation). Reference forward velocity of 5.0 m/s was commanded during this flight test.

conditions and validate whether the proposed compensation mechanism rejects wind disturbances. Experimental flight tests were performed in windy conditions using the augmented flight controller with the compensation mechanism presented in Section III.

To compare the flight control performance with and without compensation in one flight, we have used an auxiliary channel on the transmitter to switch between the augmented controller and the baseline controller during the flight tests. More than 25 flight tests were performed with the augmented flight controller under different wind speeds, and some experimental results in windy conditions are shown in Fig. 6. These results demonstrate the effectiveness of the proposed system for rejecting wind disturbances along the x-axis and improving flight control performance during hovering in windy conditions (see Fig. 6(a)). This shows a clear difference in position

error with and without compensation during hover flight.

Fig. 6(b) shows a sample of typical forward flight in windy conditions using the augmented flight controller with the compensation mechanism. The maximum tracking error for this forward flight is about 4.0 m, and the RMSE was recorded as 1.534 m, which shows some improvement in tracking the trajectory in windy conditions compared to the results in Fig. 5(b).

REMARK 3: Generally, it is difficult to assess the improvement in trajectory tracking during forward flight with relatively high velocities. This is because the dominant component of tracking error is due to latencies in GPS measurements and to the response time of the inner-loop controller, especially during the transient or acceleration phase. Therefore, higher accelerations and/or higher forward velocities will result in higher tracking errors.

A statistical analysis of the position error in the longitudinal x-axis for several flight tests and different wind speeds is given in Table I. This includes a comparison of the RMSE and maximum position errors for closed-loop flights with and without the compensation mechanism. It is clearly evident from this table that the position accuracy of the baseline controller can be improved in windy conditions by using a simple feed-forward compensation mechanism, without retuning the controller gains or using any complex flight controller. For example, the improvement in the error RMSE for hover 3 is about 63.41%, and the improvement in the error RMSE for tracking 2 is about 65.17%.

V. FORWARD FLIGHT CONTROL USING ONBOARD AIRSPEED MEASUREMENTS ONLY

The onboard airspeed measurements can be directly used by the outer-loop controller to control the forward motion of rotorcraft without GPS aid. This is a useful capability that can be used to serve two important purposes: 1) act as a backup system to control the vehicle forward motion in case the GPS signal is lost; and 2) regulate the vehicle airspeed to its recommended value to maximize the vehicle performance and safety during forward/cruise flights and to remain within its flight envelope, especially in windy conditions.

Flight tests have been performed in an outdoor environment, where the Helix8 RUAS was tasked to perform a cruise/forward flight with a desired airspeed of 5.0 m/s. In these experiments, vertical motion is controlled using data from a barometer altimeter (no GPS), while lateral motion is still controlled using GPS data. Fig. 7 shows experimental results from a forward flight using an airspeed-based velocity controller. It can be seen from this figure that the desired airspeed was tracked reliably and with enough accuracy to allow the rotorcraft to control its forward motion and travel a distance of about 60.0 m using only an airspeed-based velocity controller along the x-axis. These results prove that airspeed data can be used for cruise flight monitoring but also in a closed-loop for forward flight control even of small RUAS traveling at moderate speeds.

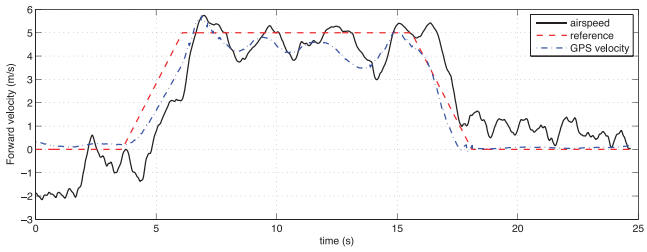

Fig. 7. Control of forward velocity using airspeed measurements only. GPS ground speed is plotted for comparison purposes only.

VI. CONCLUSION

A low-cost system for online estimation of airspeed onboard small unmanned rotorcraft is presented in this paper. This includes sensors integration, software implementation, and experimental validation using a small multirotor UAS. These real-time airspeed measurements provide valuable information and can be used for different purposes and applications. In this paper, we investigated the use of onboard airspeed measurements for two important applications: 1) online wind speed estimation along the flight direction and compensation of wind disturbances, thereby improving the flight control performance of small rotorcraft in windy conditions; and 2) closed-loop control of forward motion using airspeed measurements only without GPS aid. The proposed system and algorithms have been extensively validated in closed-loop flight tests under different weather conditions.

In its current implementation, the system is limited to wind compensation and/or non-GPS flight control in the longitudinal direction only. Although this is enough for many real-world applications, where aircraft and rotorcraft generally fly forward along their longitudinal x-axis, the system can be extended to other directions. Indeed, future work in this area will focus on extending the current system capabilities to enable wind compensation and non-GPS flight control in the three directions (i.e., longitudinal, lateral, and vertical).

BILAL ARAIN,
Australian Research Centre for Aerospace Automation
Queensland University of Technology
22-24 Boronia Road,
Eagle Farm Brisbane, Queensland 4009 Australia
E-mail: (arain.bilal@gmail.com)

FARID KENDOUL,
CSIRO Autonomous Systems Laboratory, Australia

REFERENCES

[1] Cho, A., Kim, J., Lee, S., and Kee, C.
Wind estimation and airspeed calibration using a UAV with a single-antenna GPS receiver and pitot tube.
IEEE Transactions on Aerospace and Electronic Systems, **47**, 1 (Jan. 2011), 109–117.

[2] van den Kroonenberg, A., Martin, T., Buschmann, M., Bange, J., and Vörsmann, P.
Measuring the wind vector using the autonomous mini aerial vehicle M2AV.
Journal of Atmospheric and Oceanic Technology, **25**, 11 (2008), 1969–1982.

[3] Bisgaard, M., la Cour-Harbo, A., and Danapalasingam, K.
Nonlinear feedforward control for wind disturbance rejection on autonomous helicopter. In
Proceedings of the IEEE International Conference on Intelligent Robots and Systems, Taipei, China, 2010, 1078–1083.

[4] Etele, J.
Overview of wind gust modelling with application to autonomous low-level UAV control. Defence R&D Canada, Ottawa, Canada, Contract Report CR 2006-221, November 2006.

[5] Martini, A., Léonard, F., and Abba, G.
Dynamic modelling and stability analysis of model-scale helicopters under wind gust.
Journal of Intelligent and Robotic Systems, **54**, 4 (2009), 647–686.

[6] Pflimlin, J.-M., Hamel, T., Soures, P., and Mahony, R.
A hierarchical control strategy for the autonomous navigation of a ducted Fan Flying Robot. In
Proceedings of the IEEE International Conference on Robotics and Automation, Orlando, FL, 2006.

[7] Yang, X., Pota, H., and Garratt, M.
Design of a gust-attenuation controller for landing operations of unmanned autonomous helicopters. In
Proceedings of the IEEE Multi-Conference on Systems and Control, Saint Petersburg, Russia, 2009.

[8] Munoz, L., Castillo, P., Sanahuja, G., and Santos, O.
Embedded robust nonlinear control for a four-rotor rotorcraft: validation in real-time with wind disturbances. In
Proceedings of the International Conference on Intelligent Robots and Systems, San Francisco, CA, 2011, 2682–2687.

Enhanced OFDM-Based Ranging Method for Space Applications

In this paper, an enhanced ranging method is proposed for an orthogonal frequency division multiplexing–based ranging system for space applications. In the proposed method, the classical multiple-signal classification algorithm is introduced and used to estimate the fractional part of the round-trip delay. Simulation results show that the proposed method can improve the estimation accuracy dramatically in the low signal-to-noise ratio regime.

I. INTRODUCTION

Radio ranging techniques play an important role in location systems, navigation systems, and so on. The general method used to measure the range between two distant points is to estimate the roundtrip delay of a signal wave. The pseudonoise (PN) ranging methods proposed in [1, 2] use a PN sequence as the signal wave. In [3], a phase ranging method is proposed that estimates the round-trip delay by measuring the phase of the received signal. To increase the estimation accuracy and measurable range in space applications, [4] proposed a novel ranging system that is developed on the basis of the orthogonal frequency division multiplexing (OFDM) signal. Although this method performs better than the PN ranging and phase ranging methods, the estimation accuracy is poor in the low signal-to-noise ratio (SNR) regime.

In this paper, we propose an enhanced ranging method for an OFDM-based ranging system in space applications. Noting that the returned signal in the frequency domain has the same structure as that of the signal received by an antenna array, we introduce the classical multiple-signal classification (MUSIC) algorithm and use it to estimate the fractional part of the round-trip delay. The MUSIC algorithm is usually used in the direction of arrival (DOA) estimation and can achieve a high estimation accuracy in the low SNR regime [5–8].

Manuscript received September 16, 2012; revised March 16, 2013; released for publication September 20, 2013.

DOI. No. 10.1109/TAES.2014.120583.

Refereeing of this contribution was handled by M. Rice.

This work was supported by the National "Eleventh Five-Year" Project of China (2012ZX03003005-003), the National Natural Science Foundation of China (BK2012738, 61372100), and Chinese 863 Program (2011AA01A105, 2012AA011401).

Authors' address: National Mobile Communications Research Laboratory, Southeast University, Nanjing 210096, China, E-mail: (sbdtt@seu.edu.cn).